



Application of *Terminalia arjuna* as potential adsorbent for the removal of Pb(II) from aqueous solution: thermodynamics, kinetics and process design

Rifaqat Ali Khan Rao^{a,*}, Amna Khatoon^a, Ahmad Ashfaq^b

^aEnvironmental Research Laboratory, Faculty of Engineering and Technology, Department of Applied Chemistry, Aligarh Muslim University, Aligarh, UP, India, Tel. +91 0571 2703167, ext. 3000; emails: rakrao1@rediffmail.com (R.A.K. Rao), amnanaseer.amu@gmail.com (A. Khatoon)

^bFaculty of Engineering and Technology, Department of Civil Engineering, Aligarh Muslim University, Aligarh, UP, India, email: ahmad_ashfaq76@yahoo.com

Received 9 December 2014; Accepted 22 August 2015

ABSTRACT

The present work explored the adsorption properties of *Terminalia arjuna* fruit powder for the removal of Pb(II) from aqueous solution. Effect of concentration, contact time, pH, adsorbent dose, and temperature were studied using batch process to optimize conditions for maximum adsorption of Pb(II). Kinetic data showed that the pseudo-second-order model was the best fit for the experimental data over a wide range of concentrations. Thermodynamic parameters (ΔH° and ΔG°) suggested endothermic and spontaneous nature of adsorption. Mean free energies at different temperatures were in between 10.1 and 14.3 kJ mol⁻¹ indicating chemical nature of adsorption process. Equilibrium isotherm data were analyzed using Langmuir, Freundlich, Temkin and Dubinin–Radushkevich (D–R) isotherms models at 30, 40, and 50°C. The breakthrough and exhaustive capacities were found to be 5 and 15 mg g⁻¹, respectively. Desorption studies were carried out by column method and 84% of Pb(II) ions were recovered when 0.05 N HCl was used. A single-stage batch adsorption design was proposed to predict the amount of adsorbent required for 98% removal of Pb(II) from different volumes of water.

Keywords: *Terminalia arjuna*; Adsorption; Thermodynamics; Breakthrough capacity; Desorption

1. Introduction

Environmental degradation is accelerating day by day due to the continuous release of various contaminants in air soil and water owing to the rapid industrialization and urbanization [1]. The most significant pollutants found in wastewater are heavy metals. They are persistent in nature and highly toxic even at ultra-trace levels [2]. Heavy metals are non-biodegrad-

able and hence they tend to accumulate in the tissues and vital organs of living organism thereby causing various diseases and long-term disorders [3]. Among the variety of heavy metals found in wastewater Pb(II) is considered to be one of the most toxic contaminants. This metal is known to cause a number of adverse effects on human health as it can accumulate in the kidney, liver, brain, bones, and muscles. Chronic toxicity occurs at blood levels of 0.4–0.6 mg L⁻¹ [4]. The maximum permissible limit assigned by World

*Corresponding author.

Health Organization (WHO) for Pb(II) in drinking water is 0.05 mg L^{-1} [5]. As reported by health organizations, Pb(II) can alter numerous metabolic body processes and induce impairment and dysfunction in the blood and cardiovascular system in human adults and particularly in children [6]. The condition of children in developing countries is quite miserable with more than 15 million of them are suffering from permanent neurological damage due to Pb(II) poisoning [7].

Some of the techniques commonly employed to remove Pb(II) from aqueous solutions include membrane filtration, ultra-filtration and reverse osmosis, and chemical precipitation of Pb(II) as the hydroxide and sulfide and ion exchange [8–13]. All these methods suffer from one or the other drawback. Some of the drawbacks include high operational cost, production of a chemical byproduct that requires further treatment, low removal efficiency, difficult implementation, etc. Adsorption is a quite attractive process for the removal of Pb(II) from aqueous solutions. Activated carbon has long been used as effective adsorbent but its high cost and difficulty in regeneration has prompted researchers to explore the adsorption properties of naturally occurring biomass as they are available in abundance, economical, easily prepared, and eco-friendly. The other advantages of using natural biomass as adsorbents are that they do not release any toxic or objectionable substance when added into water or wastewater for treatment in comparison to synthetic and nano-adsorbents where the chances of leaching of metals of whom they are synthesized cannot be ignored. Various studies on Pb(II) removal from aqueous solution using natural adsorbents include activated carbon prepared from biomass materials [14], rice husks [15,16], barley straws [17], maize husks [18], sawdust [19,20], sugarcane bagasse [21], coriander seed [22], neem oil cake (NOC) [23], modified water hyacinth [24], castor leaf powder [25], green alga [26], *Laminaria japonica* [27], etc.

The objective of the present work is to explore the adsorption properties of *Terminalia arjuna* fruit for the removal of Pb(II) from aqueous solution. *T. arjuna*, commonly known as arjuna or arjun belongs to the family Combretaceae. It is a large evergreen tree and the height reaches up to 60–80 feet. It is mainly found in the greater parts of Indian peninsula. Flowering begins in April and extends to May with the fruit ripening the following February–May. The diameter of fruit is 1–1.5 inch with 5–7 longitudinal lobes. The fruit of *T. arjuna* is found to possess large number of phytochemicals, namely arjunone, methyl oleanolate, gallic acid, hentriacontane, arachidic stearate, ellagic acid, arjunic acid, β -sitosterol, friedelin, myristil oleate

[28]. In comparison to other commonly used medicinal plants, bark of *T. arjuna* contains a very high level of flavonoids. Some of the flavonoids obtained from its bark include pelargonidin, arjunolone, flavones, kempferol, quercetin, and bicalcin. The bark, leaves, and fruit possess glycosides, large quantities of flavonoids, tannins, and minerals [29]. Phenolic contents of these parts are also quite high (72.0 – 167.2 mg kg^{-1}) [30].

2. Materials and methods

2.1. Preparation of adsorbent

T. arjuna nuts were collected locally from university campus of Aligarh, UP, India in the month of May. Collected nuts were washed several times with distilled water in order to remove adhering dirt and dust particles and then dried in an open air oven at 60°C for 48 h. The dried fruits were grounded and sieved through 300–150 μm of screen size using standard ASTM sieves. The sieved sample was again washed repeatedly with double-distilled water (DDW) to remove color. The biomass was finally dried at 60°C for 24 h in oven and was stored in an airtight bottle for further study.

2.2. Chemicals and reagents

All chemicals and reagents used were of analytical grade (A.R) and were obtained from Merck, Germany. They were used as such without further purification. Stock solution of Pb(II) ($1,000 \text{ mg L}^{-1}$) was prepared by dissolving appropriate amount of lead nitrate salt in required volume of DDW. Working standard solutions of Pb(II) of desired concentrations were obtained by diluting the stock solution.

2.3. Characterization of adsorbent

To investigate the surface morphology of the adsorbent before and after Pb(II) adsorption, scanning electron microscopy (SEM) of gold-coated samples were carried out on a carbon tape in a JSM-6510LV scanning electron microscope (JEOL, Japan) at an accelerating voltage of 20 kV and magnification of 7,500. The type of binding groups present on the adsorbent were examined by Fourier transform infrared (FTIR) analysis with pellets prepared by mixing spectroscopic grade potassium bromide (KBr) and the adsorbent in the ratio of 4:1. The spectra were recorded in the range of 400–4,000 wave numbers (cm^{-1}) in the diffuse reflectance mode at a resolution of 4 cm^{-1} in KBr pellets. The determination of elemental composition of the adsorbent before and

after Pb(II) adsorption was carried out using the Oxford Instruments INCA X-sight energy dispersive X-ray (EDX) spectrometer equipped SEM.

2.4. Determination of active sites

Active sites present on the surface of the adsorbent were determined by acid–base titration method as described by Ghodbane et al. [31].

2.5. Batch adsorption studies

The adsorption studies were investigated by batch process. 0.2 g of adsorbent was placed in a 250-mL standard conical flask containing 20 mL of Pb(II) solution of desired concentration. The conical flask was taken out from shaker at a predetermined time interval and the mixture was filtered using Whatman filter paper No. 1. The final concentration of Pb(II) in filtrate was then determined by atomic absorption spectrophotometer (AAS). The % adsorption of Pb(II) and the adsorption capacity, q_e (mg g^{-1}) of the adsorbent at equilibrium were determined using the following relationships:

$$\% \text{ Adsorption} = \left(\frac{C_o - C_e}{C_o} \right) \times 100 \quad (1)$$

$$\text{Adsorption capacity } (q_e) = \left(\frac{C_o - C_e}{m} \right) \times V \quad (2)$$

where C_o and C_e are the initial and final Pb(II) concentrations, respectively; V is the volume of the solution (L) and m is the mass of the adsorbent (g).

2.6. Effect of contact time

A series of 250-mL conical flasks, each containing 0.2 g of adsorbent and 20 mL solution of Pb(II) of concentration 50 mg L^{-1} , were shaken in a temperature-controlled shaker incubator. The flasks were taken out at a predetermined time interval and were filtered using Whatman filter paper No. 1. The concentration of Pb(II) in each filtrate was then determined by AAS and the amount of Pb(II) adsorbed in each case was determined as described above.

2.7. Effect of pH

The effect of pH was studied in the pH range of 1–10. The experiments were carried out in batch mode as follows: 40 mL of Pb(II) solution of concentration

50 mg L^{-1} was taken in a beaker. The pH adjustment of solution was done by adding either 0.1 N HNO_3 or 0.1 N NaOH . The concentration of Pb(II) in this solution was then determined (initial concentration). 20 mL of this solution was taken in conical flask and treated with 0.2 g of adsorbent. The mixture was shaken in a shaker incubator. After equilibrium, the mixture was filtered and the final concentration of Pb(II) in filtrate was determined by AAS. The final or equilibrium pH (pH_f) was also recorded using pH meter. In order to investigate the effect of electrolyte (KNO_3), same procedure was followed as described above using Pb (II) solution (50 mg L^{-1}) prepared in 0.1 N KNO_3 .

2.8. Point of zero charge

The zero surface charge characteristic of the adsorbent was determined by solid addition method [32]. The experiment was carried out as follows: 15 mL of 0.1 N KNO_3 solution was placed in a series of 100-mL conical flasks. The initial pHs (pH_i) of the solutions was roughly adjusted between 1 and 10 by adding either 0.1 N HNO_3 or 0.1 N NaOH solutions. The total volume of the solution in each flask was made up to 20 mL by adding KNO_3 solution of the same strength. The initial pH values (pH_i) of the solutions were accurately measured using pH meter. Thereafter, 0.2 g of adsorbent was transferred into each flask and the mixture was allowed to equilibrate for 24 h with intermittent manual shaking. After equilibrium, solutions were filtered and the final pH (pH_f) of the supernatant liquid was recorded. The point of zero charge (PZC) curves was obtained by plotting difference between the initial pH (pH_i) and final pH (pH_f), i.e. ΔpH values against pH_i . The point of intersection of the resulting curve with the abscissa, at which $\Delta\text{pH} = 0$, gave the pH_{PZC} .

2.9. Effect of adsorbent dose

To study the effect of adsorbent dose on the adsorption of Pb(II), a series of 250-mL conical flasks each containing a fixed volume of Pb(II) solution (20 mL) of concentration 50 mg L^{-1} were treated at 30°C with varying amount of adsorbent (0.1–1.0 g). The flasks were kept in a shaker incubator. The solutions were then filtered after 24 h. The amount of Pb(II) in the filtrate was then determined by AAS.

2.10. Breakthrough studies

0.5 g of adsorbent was accurately weighed and transferred into a glass column (0.6 cm internal

diameter) with glass wool support. 250 mL of Pb(II) solution with initial concentration (C_o) of 50 mg L^{-1} was then passed through the column with a flow rate of 1 mL min^{-1} . Bed height was 3.5 cm, bed volume was 0.99 cm^3 , and L/D ratio was 5.83. The concentration of Pb(II) (C_e) in each fraction was then determined by AAS. The breakthrough curve was obtained by plotting C_e/C_o vs. volume of the effluent.

2.11. Desorption studies

The exhausted column after the determination of breakthrough capacity was used to study the desorption behavior. The column was washed several times with DDW in order to remove traces of Pb(II) ions remained unadsorbed. 0.05 N HCl was then used as desorbing solution for the desorption of Pb(II) ions from adsorbent. The solution was passed through the column at a flow rate of 1 mL min^{-1} and the effluent was collected in 10 mL fractions. Each fraction was then analyzed by AAS for determining the amount of Pb(II) desorbed.

3. Results and discussion

The adsorption of various heavy metal ions on *T. arjuna* fruit powder (TAFP) was investigated under identical conditions of temperature, concentration, and pH and it was observed that the adsorbent showed highest affinity toward Pb(II) followed by Zn(II), Ni(II), Cd(II), Cr(VI), and Cu(II) (Fig. 1). The maximum adsorption of Pb(II) might be due its smaller hydrated ionic radius (4.01 \AA) than the other metal ions being investigated in the present study [33].

The monolayer adsorption capacity of Pb(II) investigated on TAFP was found to be higher than many other adsorbents reported earlier (Table 1).

3.1. Characterization of adsorbent

3.1.1. SEM analysis

SEM imaging was performed to examine the surface morphology of TAFP before and after adsorption of Pb(II). Scanning electron micrographs are depicted in Fig. 2. In both the cases, surface of the adsorbent appeared to be irregular and porous and thus revealing amorphous nature of adsorbent. The surface of adsorbent before adsorption of Pb(II) appeared to be less dense, while after adsorption it became denser, showing adherence of Pb(II) on the surface in the form of white patches.

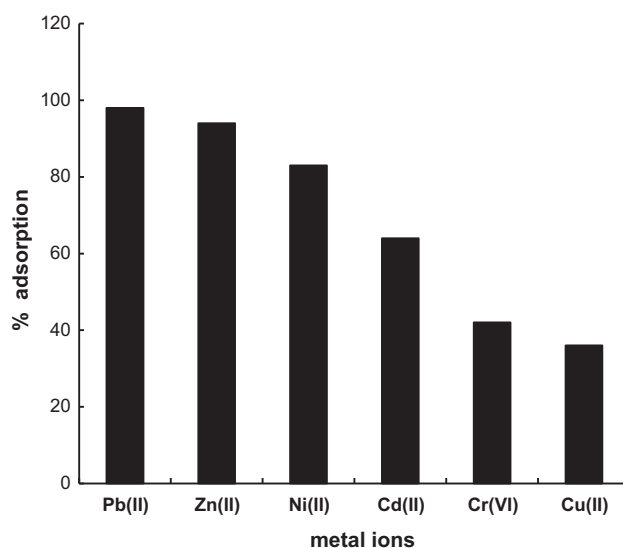


Fig. 1. Percent adsorption of heavy metal ions from aqueous solution onto TAFP (conditions: adsorbent dose = 0.2 g; temp. = 30°C).

3.1.2. EDX analysis

EDX spectra of TAFP before and after adsorption of Pb(II) are illustrated in Fig. 3. Spectrum before adsorption clearly indicated the peak for the presence of carbon and oxygen as major constituents. EDX spectra after adsorption showed a peak of Pb(II) confirming adsorption of Pb(II) on to the surface of adsorbent. The weight % of different constituents obtained from EDX analysis before and after Pb(II) adsorption is reported in Table 2. Moreover, before and after adsorption no characteristic peaks were observed for any impurities.

3.1.3. FTIR spectroscopy

FT-IR analysis was carried out to identify characteristic functional groups present in TAFP and the spectra of the adsorbent before and after adsorption of Pb(II) are shown in Fig. 4(a) and (b). The broad and strong absorption peak at $3,446 \text{ cm}^{-1}$ indicated the presence of OH group [43]. The sharp and intense peak at $1,642 \text{ cm}^{-1}$ was aroused due to stretching vibrations of C=C [44]. The band at $1,429 \text{ cm}^{-1}$ indicated the presence of $-\text{COO}^-$ group [5]. The broad peak at $1,122 \text{ cm}^{-1}$ was due to C–O stretching vibrations [45]. The broad and short peak observed at 601 cm^{-1} might be due to M–O (metal-oxide) bond as metal oxides generally give absorption bands below $1,000 \text{ cm}^{-1}$ arising from interatomic vibrations [45,46]. FTIR spectra of the adsorbent after adsorption of Pb(II) (Fig. 4(b)) showed shift in some of the absorption

Table 1

Comparison of monolayer adsorption capacity (q_m) of various adsorbents toward Pb(II) reported in the literature

Adsorbents	Monolayer adsorption capacity (q_m) (mg g ⁻¹)	Refs.
Barley straw	23.20	[17]
Ball clay	03.52	[34]
Coir	18.90	[35]
Chemically modified oil palm fruit fiber	05.58	[36]
coral	01.14	[37]
Egg shell	04.74	[37]
Hazelnut shells	16.23	[38]
Olive cake	19.53	[38]
Rice husk	11.40	[38]
<i>Imperata cylindrica</i> leaf powder	13.50	[39]
Oil palm shell	03.39	[40]
Orange peels	01.22	[41]
<i>Pinus sylvestris</i>	09.71	[42]
<i>Terminalia arjuna</i> fruit powder	27.39	Present study

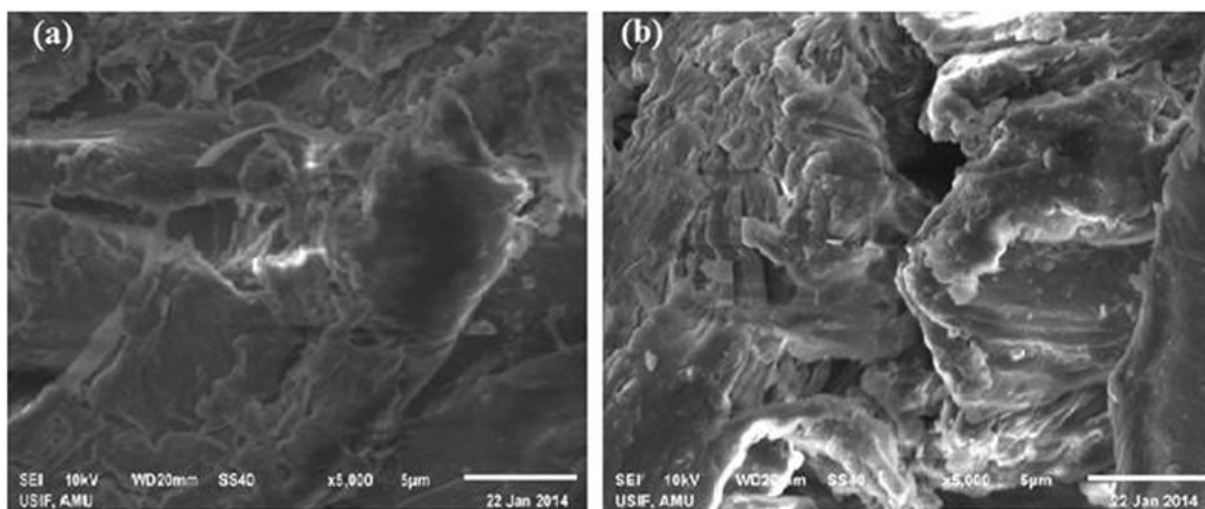


Fig. 2. SEM micrograph of TAFP (a) before and (b) after adsorption of Pb(II) (Magnification: 5,000× in both case).

bands toward lower frequencies. Shifting of bands to lower frequencies indicates bond weakening, while a shift to higher frequencies indicates an increase in bond strength [45,47]. Shifting of the peaks was observed in the region close to 1,642, 1,122 and 601 cm⁻¹. These peaks were shifted to 1,629, 1,068, and 587 cm⁻¹, respectively. The disappearance of peak at 1,429 cm⁻¹ indicated the strong interaction of Pb(II) with COO group.

3.2. Determination of active sites

The total active sites matching the carboxylic and phenolic sites were neutralized using alkaline

solutions of 0.1 N NaOH, 0.1 N NaHCO₃, and 0.1 N Na₂CO₃. The total of carboxylic and phenolic sites as estimated by the method described by Ghodbane et al. [31] is reported in Table 3.

3.3. Effect of initial Pb(II) concentration and contact time

The effect of initial concentration of Pb(II) was studied in the concentration range of 10–100 mg L⁻¹ (Fig. 5). A usual phenomenon of increase in adsorption capacity with an increase in the initial Pb(II) concentration was observed which may be attributed to the increased concentration gradient between the bulk solution and adsorbent surface thereby lowering the

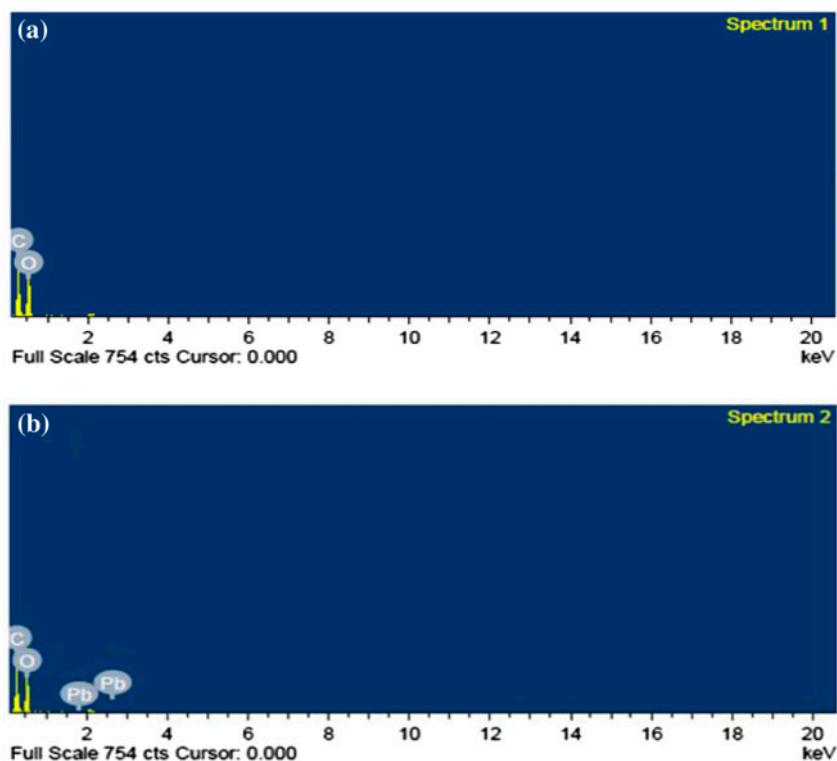


Fig. 3. EDX spectra of TAFP (a) before and (b) after adsorption of Pb(II).

Table 2
EDX analysis of TAFP before and after adsorption of Pb(II)

Elements	Before adsorption		After adsorption	
	Weight (%)	Atomic (%)	Weight (%)	Atomic (%)
C	45.46	52.61	44.60	52.06
O	54.54	47.39	54.64	47.88
Pb	–	–	0.76	0.05
Total	100.00	100.00	100.00	100.00

resistance to mass transfer of Pb(II) from aqueous to solid phase [23,48]. The maximum adsorption of Pb(II) at equilibrium was found to be 0.95, 1.92, 4.91, 5.90, 7.85, and 9.80 mg g⁻¹ at initial Pb(II) concentrations of 10, 20, 50, 60, 80, and 100 mg g⁻¹, respectively. The contact time required to reach equilibrium was found to be dependent on initial Pb(II) concentration up to 80 mg L⁻¹ and then became independent of concentration (Fig. 5). This was due to the fact that empty adsorbent sites adsorbed Pb(II) ions rapidly at lower concentration but at higher concentration adsorption of Pb(II) ions occurred by diffusion (slower step) into the inner sites of the adsorbent. The equilibrium time of 5–30 min investigated in the present work was

much shorter than many other adsorbents reported earlier for Pb(II) adsorption (Table 4).

3.4. Effect of pH

The effect of pH on the adsorption of Pb(II) was investigated in the pH range of 1–10. The results are shown in Fig. 6. The % adsorption of Pb(II) was least at pH 2 and increased with increasing pH, reached maximum (96%) at pH 4, but beyond pH 4 the % adsorption decreased slowly up to pH 10. The effect of pH on the adsorption of Pb(II) can be explained on the basis of the initial pH (pH_i) of the solution, final or equilibrium pH (pH_f), surface charge of the

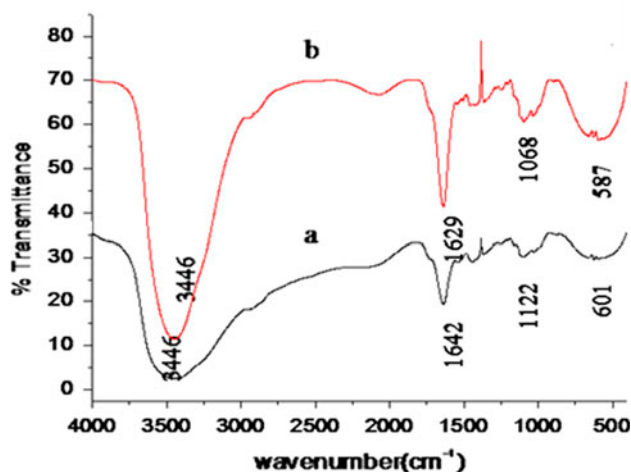


Fig. 4. FTIR spectra of TAFP (a) before and (b) after adsorption of Pb(II).

Table 3
Concentration of active sites onto the surface of TAFP

Sites	Concentration (meq g ⁻¹)
Carboxylic	0.3
Phenolic	0.15

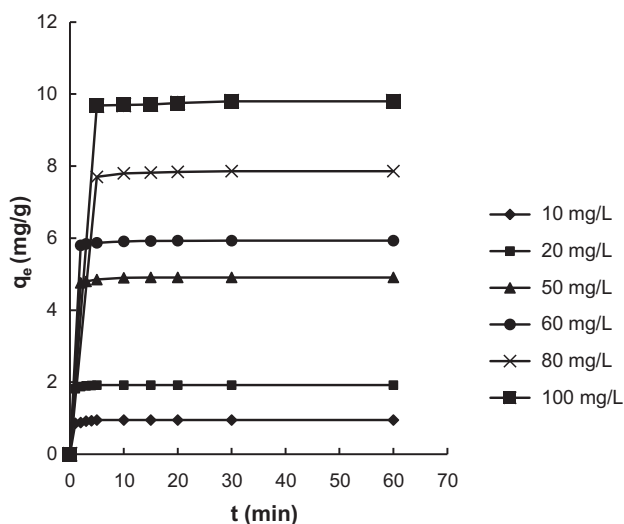
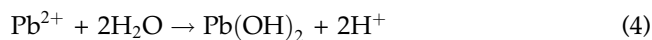


Fig. 5. Effect of contact time on the adsorption of Pb(II) onto TAFP at different concentrations (conditions: pH 4; adsorbent = 0.2 g; temp. = 30°C).

adsorbent, speciation of the metal ions in the solution [53] and also on the basis of pK_a values of major constituents that is carboxylic acid and phenols

(Table 3). At $pH < 4$ COOH group remained u-dissociated, but at $pH > 4$ the ionization of COOH produces negatively charged COO^- which interacts Pb^{2+} ions easily. Fig. 6 showed that when initial pH (pH_i) was adjusted to 1, pH_f remained almost constant and the adsorption of Pb(II) was least (10%) because of the electrostatic repulsion between positively charged adsorbent surface and positively charged Pb^{2+} ions; since, adsorbent surface was protonated due to the presence of excess H^+ ions [54,55]. When pH_i was adjusted to 2, the adsorption of Pb(II) increased to 42%, possibly due to a little less competition of Pb^{2+} with H^+ ions. However, when pH_i was adjusted to 4, the pH_f value increased to 6 at equilibrium and at the same time, the adsorption of Pb(II) increased to maximum (96%) as a result of the adsorption of Pb^{2+} ions along with H^+ ions. When pH_i was further increased to 6, the pH_f remained almost same ($pH_f = 6.5$) but adsorption of Pb(II) decreased slightly (95%). A similar trend continued when pH_i was further increased to 8 and 10 and adsorption of Pb(II) decreased to 84% and pH_f also reduced to a value of 7.5 (Fig. 6). The decrease in the equilibrium pH (pH_f) and adsorption of Pb(II) at $pH > 6$ can be explained on the basis of Pb(II) speciation at different pH values. Pb(II) existed in the form of Pb^{2+} at (pH 2–4); $Pb(OH)^+$ (pH 4–6); $Pb(OH)_2$ (pH 6–10); and $Pb(OH)_3^-$ (pH 10–12) [53,56]. It can therefore be concluded that Pb(II) was adsorbed as Pb^{2+} ions up to pH 4 and above this pH, Pb(II) was adsorbed in the form of various Pb(II) hydroxide species [22,57] in the form of microprecipitation. Further, the formation of hydroxide species of Pb(II) started above pH 6; hence, pH_f decreased due to excess H^+ ions remaining in the solution.



Maximum adsorption observed at pH 4 might be due to the fact that pK_a values of various carboxylic acids lie in the range of 3–5 [58] like pK_a value of COOH in gallic acid (which is one of the major constituents of TAFP) is 4.26 [59] which confirmed the maximum adsorption of Pb(II) at pH 4.

The effect of electrolyte (KNO_3) on the adsorption of Pb(II) was also studied and it was found that adsorption decreased in the presence of 0.1 N KNO_3 . The effect of electrolyte was more pronounced below pH 4 (Fig. 6) but at pH 4 and above, the adsorption of Pb(II) was not affected perhaps due to the fact that

Table 4
Comparison of equilibrium time for the adsorption of Pb(II) onto various adsorbents

Adsorbents	Equilibrium time (min)	Conc. (mg L ⁻¹)	Refs.
Coriander seed	60–120	50–70	[22]
Green alga	60	10	[26]
Sugarcane bagasse	120	100	[49]
<i>Mentha piperita</i> treated carbon	180	50	[50]
<i>Penicillium oxalicum</i>	120	100	[51]
<i>Spirodela polyrhiza</i> (L) Schleiden biomass	72	100	[52]
<i>Terminalia arjuna</i> fruit powder	5–30	10–100	Present study

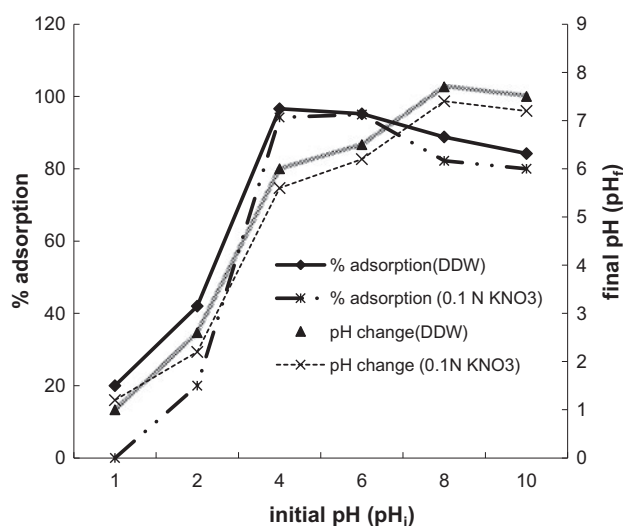


Fig. 6. Effect of pH and electrolyte on the adsorption of Pb(II) onto TAFP (conditions: adsorbent = 0.2 g; Pb(II) = 50 mg L⁻¹; temp. = 30°C).

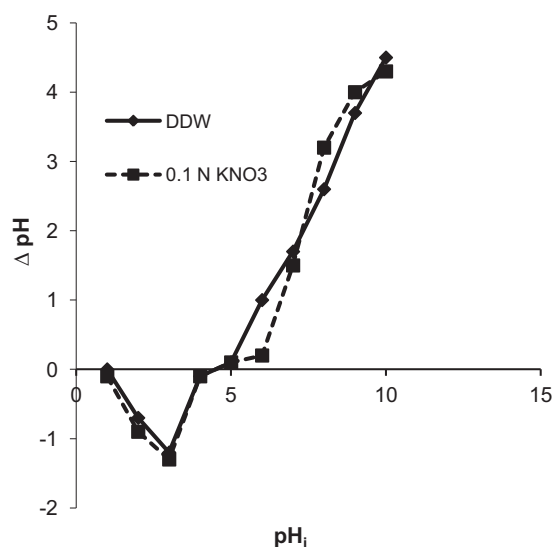


Fig. 7. Point of zero charge.

below pH 4, both H⁺ and K⁺ ions screen the electrostatic attraction between negatively charged adsorbent surface and positively charged Pb(II) ions but above pH 4, the effect of H⁺ ions (extremely low concentration) was reduced to much extent and hence adsorption of Pb(II) was not much influenced in the presence of electrolyte alone. The pHPZC (point of zero charge) of the adsorbent surface was found to be 4 (Fig. 7), indicating that adsorbent surface was positive at pH < 4; neutral at pH 4, and negatively charged at pH > 4 [55] and therefore maximum adsorption of Pb(II) was observed at pH 4.

3.5. Effect of adsorbent dose

The effect of adsorbent dose on adsorption capacity and percent adsorption of Pb(II) by varying the dose of TAFP is shown in the Fig. 8. Percent

adsorption increased while adsorption capacity, q_e (mg g⁻¹) decreased when adsorbent dose increased from 0.1 to 1.0 g. This increase in the percent adsorption of Pb(II) might be due to the fact that on increasing the adsorbent dose, number of sites available for adsorption also increased [45,60]. The maximum adsorption of Pb(II) was about 99.4% at 1 g of dose. The decrease in adsorption capacity with an increasing adsorbent dose might be due to the fact that at lower adsorbent dose, almost all the adsorption sites are saturated by the Pb(II) uptake [61] but at higher adsorbent dose, the adsorption site would be excessive for the adsorption reaction since the concentration of Pb(II) as well as the volume of the solution are constant. Additionally, a higher adsorbent dose can cause aggregation of the adsorbent particle, leading to the decline in total surface area. Thus, amount of Pb(II) adsorbed per unit mass of adsorbent was decreased [62].

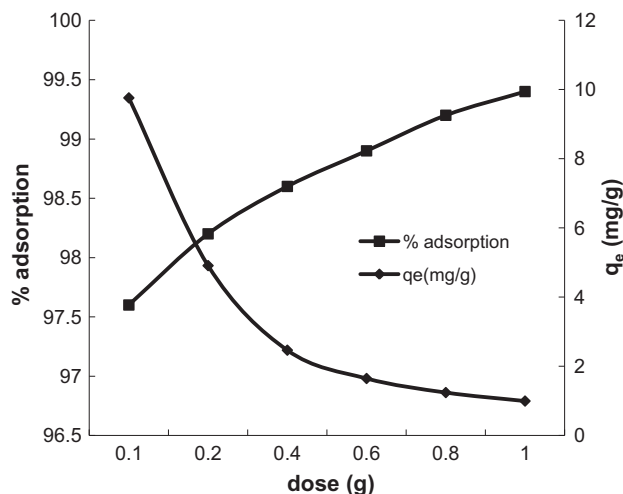


Fig. 8. Effect of doses on the adsorption of Pb(II) onto TAFP (conditions: Pb(II) = 50 mg L⁻¹; pH 4; temp. = 30°C).

3.6. Adsorption isotherms

The equilibrium adsorption isotherm is fundamentally very crucial in designing adsorption systems. In general, an adsorption isotherm is an invaluable curve describing the phenomenon governing the retention (or release) or mobility of the adsorbate from the aqueous phase to a solid phase at constant temperature and pH [63–65]. The Langmuir, Freundlich, Temkin, and Dubinin–Radushkevich (D–R) models were used to fit the experimental data for the adsorption of Pb(II) at 30, 40, and 50°C. The results obtained are reported in Table 5. In order to evaluate the fitness of the data, the values of the correlation coefficient (R^2) were evaluated for each model. Langmuir adsorption isotherm describes quantitatively the formation of monolayer on the surface of the adsorbent. The model assumes uniform energies of adsorption onto the surface and no transmigration of adsorbate in the plane of the surface [66]. The linear form of the Langmuir model may be written as:

$$\frac{1}{q_e} = \frac{1}{q_m} \times \frac{1}{b} \times \frac{1}{C_e} + \frac{1}{q_m} \quad (5)$$

where C_e is the equilibrium concentration of Pb(II) in the solution (mg L⁻¹), q_e is the amount of Pb(II) adsorbed per unit weight of adsorbent (mg g⁻¹), q_m is the amount of Pb(II) required to form a monolayer (mg g⁻¹), or the maximum monolayer adsorption capacity, and b is a constant related to the energy of adsorption (L mg⁻¹). The values of b and q_m can be calculated from the slope and intercept of the linear

plots of $1/q_e$ vs. $1/C_e$ at different temperatures (Figure not shown). The coefficient b in Langmuir equation is a measure of the stability of the complex formed between metal ions and adsorbent under specified experimental conditions [23,67]. The data obtained from the model were best fitted at 30°C as indicated by high correlation coefficient value ($R^2 = 0.999$) (Table 5).

Freundlich adsorption isotherm is commonly used to describe the adsorption characteristics on the heterogeneous surface [66,68]. The linear form of the Freundlich model can be written as:

$$\log q_e = \log K_F + \frac{1}{n} \log C_e \quad (6)$$

where K_F and n are the Freundlich constants. The constant K_F (mg g⁻¹) (L mg⁻¹)^{1/n} is an approximate indicator of adsorption capacity, while $1/n$ is a function of the strength of adsorption in the adsorption process [69]. The data obtained from this model indicated that the values of K_F and n increased as the temperature increased from 30 to 50°C (Figure not shown). The values of n between 1 and 10 indicated favorable adsorption [70]. The data also revealed that Freundlich isotherm was best obeyed at 30°C ($R^2 = 0.999$).

The Temkin isotherm contains a factor that explicitly taking into the account of adsorbent–adsorbate interactions. The model assumes that heat of adsorption (function of temperature) of all molecules in the layer would decrease linearly, rather than logarithmic with coverage by ignoring the extremely low and large value of concentrations [66]. The linear form of the Temkin equation can be written as:

$$q_e = \left(\frac{RT}{b}\right) \ln A + \left(\frac{RT}{b}\right) \ln C_e \quad (7)$$

Or,

$$q_e = B \ln A + B \ln C_e \quad (8)$$

where $(RT/b) = B$, R is the universal gas constant (J mol⁻¹ K⁻¹), T is the absolute temperature (K), and b is a constant. The quantities A (g L⁻¹) and B (J mol⁻¹) are Temkin constants related to the adsorption potential and the heat of adsorption, respectively. The values of A and B can be calculated from the slope and intercept of the plot of q_e vs. $\ln C_e$ (Figure not shown). The data obtained from the Temkin model (Table 5) indicated that this model was best fitted at 30°C ($R^2 = 0.991$).

Dubinin–Radushkevich isotherm is generally applied to express the adsorption mechanism with a

Table 5
Adsorption isotherm parameters at different temperatures.

Isotherm	Parameters	30 °C	40 °C	50 °C
Langmuir	b (L mg ⁻¹)	0.2743	1.0556	2.3115
	q_m (mg g ⁻¹)	27.390	13.850	11.820
	R^2	0.9993	0.8795	0.9506
Freundlich	K_F (mg g ⁻¹) (L mg ⁻¹) ^{1/n}	5.8425	7.0372	8.3291
	n	1.3450	1.698	2.2230
	R^2	0.9994	0.9031	0.9766
Temkin	A (L g ⁻¹)	3.105	5.873	14.546
	B (J mol ⁻¹)	5.264	4.108	3.1620
	R^2	0.9917	0.8481	0.9397
D-R	q_m (mol g ⁻¹)	2.967×10^{-3}	1.324×10^{-3}	0.562×10^{-3}
	β (mol k ⁻² J ⁻²)	4.896×10^{-9}	3.608×10^{-9}	2.441×10^{-9}
	E (kJ mol ⁻¹)	10.106	11.772	14.312
	R^2	0.9996	0.9021	0.9704

Gaussian energy distribution onto a heterogeneous surface [66,71,72]. The linear form of this equation is represented as:

$$\ln q_e = \ln q_m - \beta \varepsilon^2 \quad (9)$$

where ε is the Polanyi potential (J mol⁻¹), q_m is the monolayer capacity (mol g⁻¹), C_e is the equilibrium concentration (mol L⁻¹), and β is a constant related to the adsorption energy (mol K⁻² J⁻²). The Polanyi potential (ε) and the mean free energy of adsorption (E , kJ mol⁻¹) can be calculated from the following equations:

$$\varepsilon = RT \ln \left(1 + \frac{1}{C_e} \right) \quad (10)$$

and

$$E = \frac{1}{(2\beta)^{1/2}} \quad (11)$$

The D-R constants q_m and β were evaluated from the linear plots of $\ln q_e$ vs. ε^2 (Fig. 9). The constant β gives an idea about the mean free energy E (kJ mol⁻¹) of adsorption. The values of E obtained lie between 8 and 16 kJ mol⁻¹ showed that the adsorption was chemical in nature [73]. The data listed in Table 5 indicated that all the above models gave a good fit to the experimental data obtained at 30 °C, with the R^2 values for all the models being greater than 0.99.

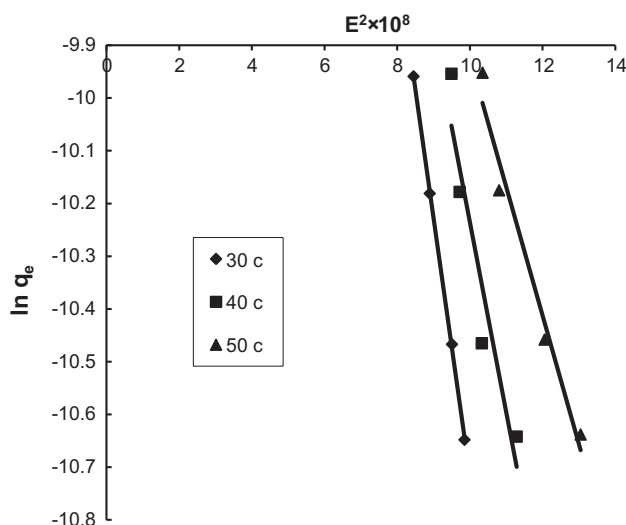


Fig. 9. D-R isotherm for the adsorption of Pb(II) onto TAFP at different temperatures.

3.7. Adsorption thermodynamics

Thermodynamic studies were conducted because they can provide information on inherent energetic changes. The effect of temperature on the adsorption of Pb(II) was studied over the temperature range of 30–50 °C. The thermodynamic parameters such as standard enthalpy change (ΔH°) and standard entropy change (ΔS°) were obtained from the Van't Hoff equation [23].

$$\log K_c = \frac{\Delta S^\circ}{2.303R} - \frac{\Delta H^\circ}{2.303RT} \quad (12)$$

ΔS° and ΔH° were calculated from the slope and intercept of linear plot of $\log K_c$ vs. $1/T$ (Fig. 10). Equilibrium constant (K_c) was calculated from the following relationship [23].

$$K_c = \frac{C_{Ac}}{C_e} \quad (13)$$

where C_{Ac} and C_e are the equilibrium concentration of Pb(II) on the adsorbent and in the solution, respectively. Standard Gibb's free energy change (ΔG°) was then calculated from the equation:

$$\Delta G^\circ = -RT \ln K_c \quad (14)$$

where T is the absolute temperature (K) and R is the gas constant ($\text{J mol}^{-1} \text{K}^{-1}$). The values obtained are listed in Table 6. The positive value of ΔH° suggested endothermic nature of adsorption of Pb(II) on TAFP. The values of ΔG° were found to be negative at all temperatures which indicated that the process was spontaneous and spontaneity increased with an increase in the temperature as indicated by a decrease in ΔG° values with an increase in the temperature. The positive value of ΔS° suggested increasing randomness at the solid/liquid interface during the adsorption process.

3.8. Adsorption kinetics

The evaluation of kinetic models is an important aspect for designing and optimization of water and

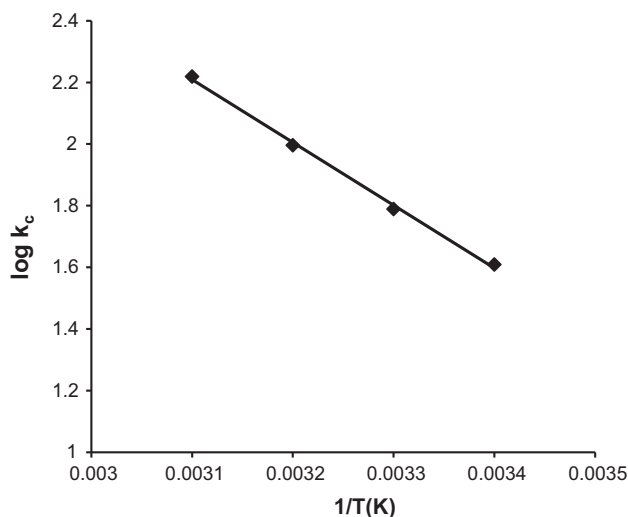


Fig. 10. Van't Hoff plot.

wastewater treatment process. Adsorption kinetic models correlate the adsorbate uptake rate [74,75]. To investigate the mechanism of adsorption and rate controlling steps, the kinetic data were analyzed using pseudo-first-order, pseudo-second-order, and intraparticle diffusion models. A pseudo-first-order kinetic model as expressed by Lagergen [76] can be written as:

$$\log (q_e - q_t) = \log q_e - \left(\frac{K_1}{2.303} \right) \times t \quad (15)$$

where q_e and q_t are the amounts of metal adsorbed (mg g^{-1}) at equilibrium and at time t , respectively, and K_1 is the pseudo-first-order adsorption rate constant (min^{-1}). A plot of $\log (q_e - q_t)$ vs. t gave straight line over a wide range of initial Pb(II) concentrations (Figure not shown). However, the values of q_e calculated ($q_{e(\text{cal})}$) from this model differed appreciably from the values of q_e obtained experimentally ($q_{e(\text{exp})}$), indicating that the adsorption process did not follow the pseudo-first-order rate equation (Table 7).

Pseudo-second-order adsorption rate equation [77] may be expressed as:

$$\frac{t}{q_t} = \frac{1}{k_2 q_e^2} + \left(\frac{1}{q_e} \right) \times t \quad (16)$$

where K_2 is the pseudo-second-order adsorption rate constant ($\text{g mg}^{-1} \text{min}^{-1}$). A plot of t/q_t vs. t gave straight line for all experimental concentrations (Fig. 11). The values of q_e and K_2 were calculated from the slope and intercept, respectively. The initial adsorption rate h ($\text{mg g}^{-1} \text{min}^{-1}$) was calculated from the relation [78].

$$h = k_2 \times q_e^2 \quad (17)$$

The values of q_e , h , K_2 , and R^2 are listed in Table 7. When the values of $q_{e(\text{cal})}$ were compared with $q_{e(\text{exp})}$, it was found that both the values were in good agreement for all experimental concentrations. Moreover, the correlation coefficient (R^2) values were also found to be very close to 1, thus it can be concluded that pseudo-second-order model was well fitted with the experimental data. It can also be seen from Table 7 that with an increase in the initial concentration of Pb(II), the rate constant (K_2) decreased. A similar observation was also reported by earlier researchers [79]. Kinetic data were also analyzed using the Weber and Morris [80] intraparticle diffusion model which can be expressed as:

Table 6
Thermodynamic parameters for the adsorption of Pb(II) onto TAFP at different temperatures

Temperature (°C)	K_C	ΔG° (kJ mol ⁻¹)	ΔH° (kJ mol ⁻¹)	ΔS° (kJ mol ⁻¹ K ⁻¹)	R^2
20	040.67	-09.027			
30	061.50	-10.376	39.002	0.163	0.9977
40	099.00	-11.958			
50	165.67	-13.722			

Table 7
Pseudo-first-order and pseudo-second-order kinetics constants for the adsorption of Pb(II) onto TAFP

Concentration (mg L ⁻¹)	$q_{e(\text{exp})}$ (mg g ⁻¹)	Pseudo-first-order kinetics			Pseudo-second-order kinetics			
		$q_{e(\text{cal})}$ (mg g ⁻¹)	k_1 (min ⁻¹)	R^2	$q_{e(\text{cal})}$ (mg g ⁻¹)	k_2 (g mg ⁻¹ min ⁻¹)	h (g mg ⁻¹ min ⁻¹)	R^2
10	0.95	0.4268	0.7026	0.7312	0.95	13.078	011.905	0.9989
20	1.92	0.5253	1.0822	0.9176	1.92	15.674	058.166	0.9999
50	4.91	0.5385	0.4214	0.9332	4.92	04.005	097.093	1.0000
60	5.90	0.2378	0.1829	0.5987	5.89	05.130	178.571	1.0000
80	7.85	0.5623	0.1829	0.8971	7.86	02.078	128.206	1.0000
100	9.80	0.4991	0.1179	0.7353	9.79	01.533	147.059	1.0000

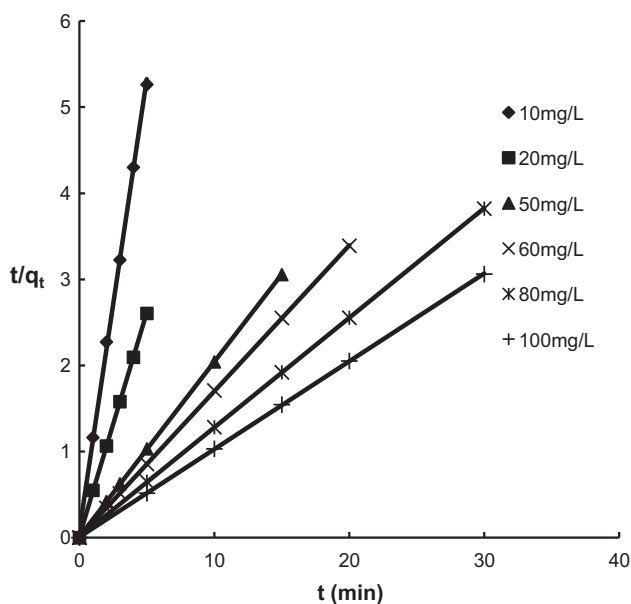


Fig. 11. Pseudo-second-order kinetics model (conditions: pH 4; adsorbent = 0.2 g; temp. = 30°C).

$$q_e = k_{id} \times t^{1/2} + I \quad (18)$$

where K_{id} is the intra-particle diffusion rate constant (mg g⁻¹ min⁻¹) and I is the intercept (mg g⁻¹) which

gives an idea about the thickness of a boundary layer, q_t is the amount of Pb(II) ions adsorbed (mg g⁻¹) at time t (min). Fig. 12 shows the plots of q_t vs. $t^{1/2}$ for different initial Pb(II) concentrations. The values of K_{id} , I , and R^2 are listed in Table 8. The deviation in the plots from origin for all concentrations indicated that intra-particle diffusion is not the only rate-controlling step, but some other processes like film diffusion and pore diffusion were also involved in the adsorption process. An increase in the intercept with an increase in the concentration indicated that boundary layer effect [81] was more pronounced with increasing Pb(II) ions concentration.

3.9. Breakthrough capacity

Determination of breakthrough capacity is an important aspect as it directly affects the feasibility and economics of the process [22,82]. Breakthrough capacity can be determined by making use of the concentration gradient between the solute adsorbed by the adsorbent and that remaining in the solution. The column is operational until the metal ions in the effluent start appearing and for practical purposes the working life of the column is over, called breakthrough point. The breakthrough curve (Fig. 13) indicated that 50.5 bed volume or 50 mL of Pb(II) solution containing 50 mg L⁻¹ initial concentration could be passed through the column without detecting Pb(II)

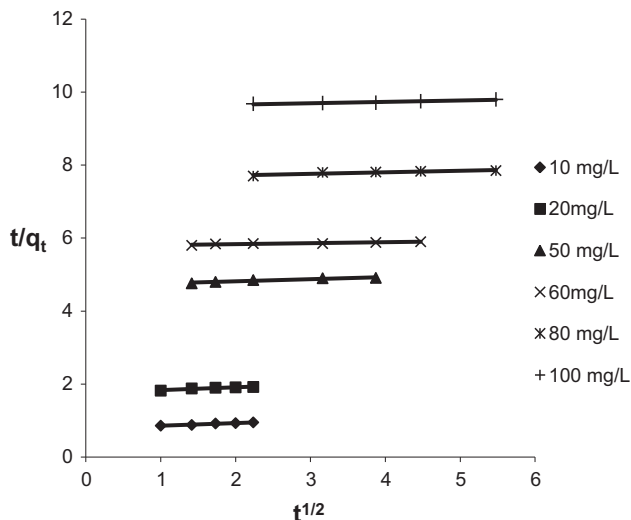


Fig. 12. Intra-particle diffusion model (conditions: pH 4; adsorbent = 0.2 g; temp. = 30°C).

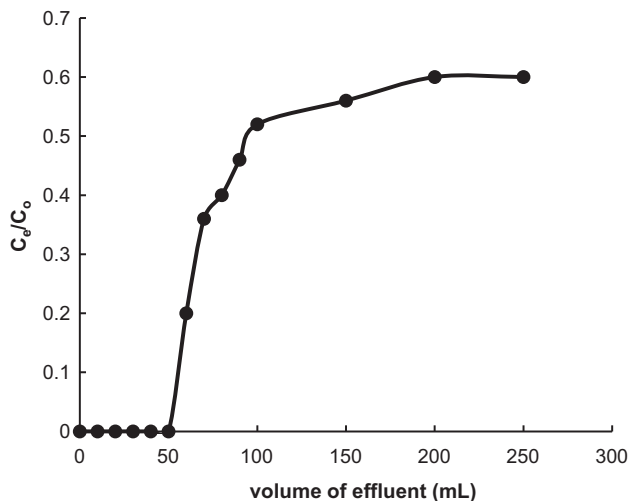


Fig. 13. Breakthrough curve (conditions: adsorbent = 0.5 g; Pb(II) = 50 mg L⁻¹; flow rate = 1 mL min⁻¹).

ions in the effluent when the bed height was 3.5 cm, bed volume was 0.99 cm³, and L/D ratio was 5.83. The breakthrough and exhaustive capacities were found to be 5 and 15 mg g⁻¹, respectively.

3.10. Desorption studies

In order to explore the practical utility of the adsorbent, desorption of Pb(II) was carried out by column process. In this study, aqueous solution of HCl was used as the desorbing agent because of its economic feasibility [83,84]. Desorption studies were carried out by using the spent column obtained from breakthrough experiment. Thus, in a breakthrough capacity experiment, it was found that a total of 7.13 mg of Pb(II) ions were retained when 250 mL of Pb(II) ion solution of concentration 50 mg L⁻¹ was passed through the column. For desorbing Pb(II) ion from TAFP, 0.05 N HCl solution was passed through this column and the effluent was collected in 10 mL fractions with a flow rate of 1 mL min⁻¹. A total of

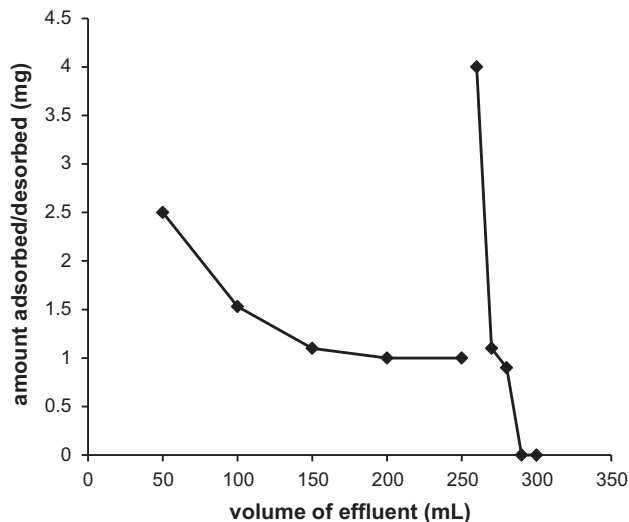


Fig. 14. Adsorption and desorption of Pb(II) by column process (conditions: adsorbent = 0.5 g; Pb(II) = 50 mg L⁻¹; flow rate = 1 mL min⁻¹).

Table 8

Intra-particle diffusion parameters for the adsorption of Pb(II) onto TAFP

Concentration (mg L ⁻¹)	k_{id} (mg g ⁻¹ min ^{-1/2})	I (mg g ⁻¹)	R^2
10	0.0751	0.7822	0.9739
20	0.0779	1.7554	0.9095
50	0.0604	4.6941	0.9174
60	0.0262	5.7795	0.8636
80	0.0428	7.6335	0.8304
100	0.0372	9.5851	0.9296

Table 9

Comparison of m/v determined experimentally and calculated from isotherms

Initial Pb(II) conc. (mg L ⁻¹)	m/v (g L ⁻¹) required for 98% removal of Pb(II)		
	Experimental	Langmuir	Freundlich
50	10.00	10.00	9.95
60	9.98	10.00	10.10
80	9.97	9.82	10.00
100	10.00	10.10	10.00

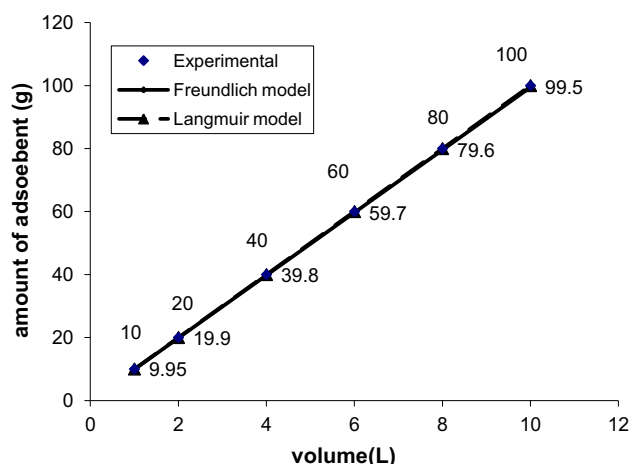


Fig. 15. Amount of adsorbent required for 98% removal of Pb(II) from different volumes of water (Langmuir and Freundlich isotherms parameter).

6.0 mg Pb(II) (84%) was recovered within 30 mL of the effluent (Fig. 14).

3.11. Designing of single stage batch adsorption system

The validity of Langmuir and Freundlich isotherms were utilized for designing the single-stage batch adsorption system. The mass balance equation for batch adsorption at equilibrium can be written as

$$v(C_o - C_e) = m \times q_e \quad (19)$$

or

$$\frac{m}{v} = \frac{(C_o - C_e)}{q_{e(cal)}} \quad (20)$$

The m/v ratio can be calculated from the above equation where $q_{e(cal)}$ is the adsorption capacity calculated from Langmuir or Freundlich isotherms at any particular equilibrium concentration (C_e) of the

adsorbate in the solution. Since the Langmuir and Freundlich models were best fitted, therefore m/v ratios from these models can be calculated as:

$$\frac{m}{v} = \frac{(C_o - C_e)}{(q_m \times b \times C_e)/(1 + b \times C_e)} \quad \text{Langmuir model}$$

and

$$\frac{m}{v} = \frac{(C_o - C_e)}{K_f \times C_e^{1/n}} \quad \text{Freundlich model}$$

Table 9 shows the amount of adsorbent (m) required for 98% removal of Pb(II) from one liter of the solution at different initial (C_o) concentrations of Pb(II). The adsorbent masses calculated from these models were found to be very close to the values determined experimentally. Fig. 15 shows the amount of adsorbent (m) required for 98% removal of Pb(II) from different volumes of aqueous solution with 50 mg L⁻¹ initial Pb(II) concentration.

4. Conclusions

The adsorption properties of *T. arjuna* have been explored using batch process. The adsorption of Pb(II) ions was pH-dependent with maximum adsorption (96%) at pH 4. The presence of electrolyte (KNO₃) in the solution has negligible effect on the adsorption of Pb(II) at pH > 4. Adsorption was fast and equilibrium reached within 30 min over a wide range of Pb(II) concentration. Kinetic data showed that pseudo-second-order rate equation was followed by the system since q_e values calculated from the model were very close to q_e determined experimentally. The fitting of the data in Langmuir, Freundlich, Temkin, and D-R isotherms indicated that these models were best fitted at 30 °C as indicated by their correlation coefficient (R^2). The maximum monolayer adsorption capacity was found to be 27.39 mg g⁻¹. The magnitude of the mean free energy indicated that adsorption of Pb(II) occurred via chemisorptions. The thermodynamic parameters ΔH° and ΔG° indicated that the adsorption process was endothermic and spontaneous. Breakthrough studies showed that 50 mL of the Pb(II)

solution of concentration 50 mg L^{-1} could be passed through the column without detecting Pb(II) ions in the effluent. Desorption studies were carried out by column method using 0.05 N HCl as desorbing solution and it was found that 84% of Pb(II) could be recovered within 30 mL of effluent. The validity of Langmuir and Freundlich isotherms was tested by designing single-stage batch adsorption system. The amount of adsorbent required for 98% removal of Pb (II) from different volumes of effluent was calculated and found to be identical to the experimental values.

Acknowledgments

Authors are thankful to the Chairman, Department of Applied Chemistry for providing research facilities. Support for this work through the Centre of Excellence in Materials Science (Nanomaterials), Department of Applied Physics, Z.H. College of Engineering and Technology, Aligarh Muslim University, Aligarh 202002, Uttar Pradesh, India is also greatly acknowledged.

Nomenclature

C_e	— equilibrium concentration of metal in the solution (mg L^{-1})
C_o	— initial concentration of metal in the solution (mg L^{-1})
q_e	— amount of adsorbate adsorbed per unit weight of adsorbent at equilibrium (mg g^{-1})
q_t	— amount of adsorbate adsorbed per unit weight of adsorbent at time t (mg g^{-1})
m	— amount of adsorbent (g)
V	— volume of metal solution (liter)
b	— Langmuir constant for energy of adsorption (L mg^{-1})
q_m	— monolayer adsorption capacity (mg g^{-1})
K_f	— Freundlich adsorption constant (mg g^{-1}) (L mg^{-1}) ^{1/n}
n	— Freundlich exponent
A	— Temkin constant for adsorption potential (g L^{-1})
B	— Temkin constant for heat of adsorption (J mol^{-1})
β	— constant related to the adsorption energy ($\text{mol K}^{-2} \text{J}^{-2}$)
ε	— Polanyi potential
E	— mean free energy (kJ mol^{-1})
R	— universal gas constant ($8.314 \text{ J mol}^{-1} \text{ K}^{-1}$)
T	— absolute temperature (K)
K_c	— equilibrium constant

C_{Ac}	— equilibrium concentration of metal on the adsorbent surface (mg L^{-1})
ΔG°	— standard free energy change (kJ mol^{-1})
ΔH°	— standard enthalpy change (kJ mol^{-1})
ΔS°	— standard entropy change ($\text{kJ mol}^{-1} \text{ K}^{-1}$)
$q_{e(\text{exp})}$	— experimental value (mg g^{-1})
$q_{e(\text{cal})}$	— calculated value (mg g^{-1})
k_1	— pseudo-first-order rate constant (min^{-1})
k_2	— pseudo-second-order rate constant ($\text{g mg}^{-1} \text{ min}^{-1}$)
h	— the initial adsorption rate ($\text{mg g}^{-1} \text{ min}^{-1}$)
k_{id}	— intra-particle diffusion rate constant ($\text{mg g}^{-1} \text{ min}^{-1}$)
I	— intercept (mg g^{-1})
t	— time (min)

References

- [1] Y.T. Zhou, H.L. Nie, C.B. Branford-White, L.M. Zhu, Z.Y. He, Removal of Cu^{2+} from aqueous solution by chitosan-coated magnetic nanoparticles modified with α -ketoglutaric acid, *J. Colloid Interface Sci.* 330 (2009) 29–37.
- [2] D. Ozdes, A. Gundogdu, B. Kemer, C. Duran, H.B. Senturk, M. Soylak, Removal of Pb(II) ions from aqueous solution by a waste mud from copper mine industry: Equilibrium, kinetic and thermodynamic study, *J. Hazard. Mater.* 166 (2009) 1480–1487.
- [3] S. Loutseti, D.B. Danielidis, A. Economouamilli, C. Katsaros, R. Santas, P. Santas, The application of a micro-algal/bacterial biofilter for the detoxification of copper and cadmium metal wastes, *Bioresour. Technol.* 100 (2009) 2099–2105.
- [4] G. Flora, D. Gupta, A. Tiwari, Toxicity of lead: A review with recent updates, *Interdiscip. Toxicol.* 5 (2012) 47–58.
- [5] R.A.K. Rao, M.A. Khan, F. Rehman, Batch and column studies for the removal of lead(II) ions from aqueous solution onto lignite, *Adsorpt. Sci. Technol.* 29 (2011) 83–98.
- [6] E.G. Moreira, I. Vassilieff, V.S. Vassilieff, Developmental lead exposure: Behavioral alterations in the short and long term, *Neurotoxicol. Teratol.* 23 (2001) 489–495.
- [7] R.F. Celeste, P.W. Choppin, J.L. Cohon, A. Huang, Health Effects of Outdoor air Pollution in Developing Countries of Asia: A literature review, HEI Publications, Cambridge, 2004, pp. 17–40.
- [8] L. Gzara, A. Hafiane, M. Dhahbi, Removal of divalent lead cation from aqueous streams using micellar-enhanced ultrafiltration, *J. Water Sci.* 13 (2000) 289–304.
- [9] Q. Chen, Z. Luo, C. Hills, G. Xue, M. Tyrer, Precipitation of heavy metals from wastewater using simulated flue gas: Sequent additions of fly ash, lime and carbon dioxide, *Water Res.* 43 (2009) 2605–2614.

- [10] A. Kongsuwan, P. Patnukao, P. Pavasant, Binary component sorption of Cu(II) and Pb(II) with activated carbon from *Eucalyptus camaldulensis* Dehn bark, *J. Ind. Eng. Chem.* 15 (2009) 465–470.
- [11] P.Y. Deng, W. Liu, B.Q. Zeng, Y.K. Qiu, L.S. Li, Sorption of heavy metals from aqueous solution by dehydrated powders of aquatic plants, *Int. J. Environ. Sci. Technol.* 10 (2013) 559–566.
- [12] L.S.G. Galindo, A.F. Almeida Neto, M.G.C. Silva, M.G.A. Vieira, Removal of cadmium(II) and lead(II) ions from aqueous phase on sodic bentonite, *Mater. Res.* 16 (2013) 515–527.
- [13] B. Sarada, M.K. Prasad, K.K. Kumar, C. Murthy, Potential use of leaf biomass, *Araucaria heterophylla* for removal of Pb²⁺, *Int. J. Phytorem.* 15 (2013) 756–773.
- [14] J. Goel, K. Kadirvelu, C. Rajagopal, V.K. Garg, Removal of lead(II) by adsorption using treated granular activated carbon: Batch and column studies, *J. Hazard. Mater.* 125 (2005) 211–220.
- [15] A. Elham, T. Hossein, H. Mahnoosh, Removal of Zn (II) and Pb(II) ions using rice husk in food industrial wastewater, *J. Appl. Sci. Environ. Manage.* 14 (2010) 159–162.
- [16] B. Singha, S. Das, Removal of Pb(II) ions from aqueous solution and industrial effluent using natural biosorbents, *Environ. Sci. Pollut. Res.* 19 (2012) 2212–2226.
- [17] E. Pehlivan, T. Altun, S. Parlayıcı, Utilization of barley straws as biosorbents for Cu²⁺ and Pb²⁺ ions, *J. Hazard. Mater.* 164 (2009) 982–986.
- [18] C.M. Zvinowanda, J.O. Okonkwo, N.M. Agyei, S.M. Van, W. Jordaan, V. Kharebe, Recovery of lead(II) from aqueous solutions by *Zea mays* tassel adsorption, *Am. J. Biochem. Biotechnol.* 6 (2010) 1–10.
- [19] A. Ahmad, M. Rafatullah, O. Sulaiman, M.H. Ibrahim, Y.Y. Chii, B.M. Siddique, Removal of Cu(II) and Pb(II) ions from aqueous solutions by adsorption on sawdust of meranti wood, *Desalination* 247 (2009) 636–646.
- [20] A. Ofomaja, E. Unuabonah, N. Oladoja, Competitive modeling for the biosorptive removal of copper and lead ions from aqueous solution by *Mansonia* wood sawdust, *Bioresour. Technol.* 101 (2010) 3844–3852.
- [21] M.Á. Martín-Lara, I.L.R. Rico, I.C.A. Vicente, G.B. García, M.C. de Hoces, Modification of the sorptive characteristics of sugarcane bagasse for removing lead from aqueous solutions, *Desalination* 256 (2010) 58–63.
- [22] R.A.K. Rao, M. Kashifuddin, Adsorption properties of coriander seed powder (*Coriandrum sativum*): Extraction and preconcentration of Pb(II), Cu(II) and Zn(II) ions from aqueous solution, *Adsorp. Sci. Technol.* 30 (2012) 127–146.
- [23] R.A.K. Rao, M.A. Khan, Removal and recovery of Cu (II), Cd(II) and Pb(II) ions from single and multimetal systems by batch and column operation on neem oil cake (NOC), *Sep. Purif. Technol.* 57 (2007) 394–402.
- [24] N.S. Ammar, H. Elhaes, H.S. Ibrahim, W. El hotaby, M.A. Ibrahim, A novel structure for removal of pollutants from wastewater, *Spectrochim. Acta, Part A: Mol. Biomol. Spectrosc.* 121 (2014) 216–223.
- [25] E.M. Amanda, S.P. Milene, O.J. Alexandre, A.U. Marco, M. Silva, J.S. Margarida, R.C. Gustavo, The reactive surface of castor leaf [*Ricinus communis* L.] powder as a green adsorbent for the removal of heavy metals from natural river water, *Appl. Surf. Sci.* 276 (2013) 24–30.
- [26] A. Sari, M. Tuzen, Biosorption of Pb(II) and Cd(II) from aqueous solution using green alga (*Ulva lactuca*) biomass, *J. Hazard. Mater.* 152 (2008) 302–308.
- [27] K.N. Ghimire, K. Inoue, K. Ohto, T. Hayashida, Adsorption study of metal ions onto crosslinked seaweed *Laminaria japonica*, *Bioresour. Technol.* 99 (2008) 32–37.
- [28] P.M. Parakh, *Terminalia arjuna* (Robx.) Wt. and Arn.: A Review, *Int. J. Pharmacol.* 6 (2010) 515–534.
- [29] R. Nema, P. Jain, S. Khare, A. Pradhan, A. Gupta, D. Singh, Preliminary phytochemical evaluation and flavonoids quantification of *Terminalia arjuna* leaves extract, *Int. J. Pharm. Phytopharmacol. Res.* 1 (2012) 283–286.
- [30] M. Bajpai, A. Pande, S.K. Tewari, D. Prakash, Phenolic contents and antioxidant activity of some food and medicinal plants, *Int. J. Food Sci. Nutr.* 56 (2005) 287–291.
- [31] I. Ghodbane, L. Nouri, O. Hamdaoui, M. Chiha, Kinetic and equilibrium study for the sorption of cadmium(II) ions from aqueous phase by eucalyptus bark, *J. Hazard. Mater.* 152 (2008) 148–158.
- [32] D.H. Lataye, I.M. Mishra, I.D. Mall, Removal of pyridine from aqueous solution by adsorption on bagasse fly ash, *Ind. Eng. Chem. Res.* 45 (2006) 3934–3943.
- [33] S.B. Chen, Y.B. Ma, L. Chen, K. Xian, Adsorption of aqueous Cd²⁺, Pb²⁺, Cu²⁺ ions by nano-hydroxyapatite: Single and multi-metal competitive adsorption study, *Geochem. J.* 44 (2010) 233–239.
- [34] V. Chantawong, N.W. Harvey, V.N. Bashkin, Comparison of heavy metal adsorptions by Thai kaolin and ball clay, *Water Air Soil Pollut.* 148 (2003) 111–125.
- [35] K. Conrad, H.C.B. Bruunhansen, Sorption of zinc and lead on coir, *Bioresour. Technol.* 98 (2007) 89–97.
- [36] A.A. Abia, E.D. Asuquo, Sorption of Pb(II) and Cd(II) ions on chemically unmodified and modified oil palm fruit fiber absorbent: Analysis of pseudo second order kinetics models, *Ind. J. Chem. Technol.* 15 (2008) 341–348.
- [37] M. Ahmad, A.R.A. Usman, S.S. Lee, S. Kim, J. Joo, J.E. Yang, Y.S. Ok, Eggshell and coral wastes as low cost sorbents for the removal of Pb²⁺, Cd²⁺ and Cu²⁺ from aqueous solutions, *J. Ind. Eng. Chem.* 18 (2012) 198–204.
- [38] M. Iqbal, A. Saeed, S.I. Zafar, FTIR spectrophotometry, kinetics and adsorption isotherms modeling, ion exchange, and EDX analysis for understanding the mechanism of Cd²⁺ and Pb²⁺ removal by mango peel waste, *J. Hazard. Mater.* 164 (2009) 161–171.
- [39] M.A.K. Hanafiah, S.C. Ibrahim, M.Z.A. Yahya, Equilibrium adsorption study of lead ions onto sodium hydroxide modified Lalang (*Imperata cylindrica*) leaf powder, *J. Appl. Sci. Res.* 2 (2006) 1169–1174.
- [40] H.L.H. Chong, P.S. Chia, M.N. Ahmad, The adsorption of heavy metal by Bornean oil palm shell and its potential application as constructed wetland media, *Bioresour. Technol.* 130 (2013) 181–186.
- [41] Z. Xuan, Y. Tang, X. Li, Y. Liu, F. Luo, Study on the equilibrium, kinetics and isotherm of biosorption of lead ions onto pretreated chemically modified orange peel, *Biochem. Eng. J.* 31 (2006) 160–164.
- [42] M. Ghasemi, M. Naushad, N. Ghasemi, Y. Khosravifard, A novel agricultural waste based adsorbent for the removal of Pb(II) from aqueous solution: Kinetics, equilibrium and thermodynamic studies, *J. Ind. Eng. Chem.* 20 (2014) 454–461.

- [43] R.A.K. Rao, S. Ikram, Sorption studies of Cu(II) on gooseberry fruit (*emblica officinalis*) and its removal from electroplating wastewater, *Desalination* 277 (2011) 390–398.
- [44] M.Z. Haque, M. Abdullah, M.U. Ali, M.Y. Ali, M.A. Al-Maruf, Investigation on *Terminalia arjuna* fruits: part I- isolation of compounds from petroleum ether fractions, *Bangladesh J. Sci. Ind. Res.* 43 (2008) 123–130.
- [45] R. Wang, Q. Li, D. Xie, H. Xiao, H. Lu, Synthesis of NiO using pine as template and adsorption performance for Pb(II) from aqueous solution, *Appl. Surf. Sci.* 279 (2013) 129–136.
- [46] K. Anandan, V. Rajendran, Morphological and size effects of NiO nanoparticles via solvothermal process and their optical properties, *Mater. Sci. Semicond. Process.* 14 (2011) 43–47.
- [47] A.D. Dwivedi, S.P. Dubey, K. Gopal, M. Sillanpää, Strengthening adsorptive amelioration: Isotherm modeling in liquid phase surface complexation of Pb (II) and Cd (II) ions, *Desalination* 267 (2011) 25–33.
- [48] Z. Aksu, D. Akpinar, Modelling of simultaneous biosorption of phenol and nickel(II) onto dried aerobic activated sludge, *Sep. Purif. Technol.* 21 (2001) 87–99.
- [49] I.A.A. Hamza, B.S. Martincigh, J.C. Ngila, V.O. Nyamori, Adsorption studies of aqueous Pb(II) onto a sugarcane bagasse/multi-walled carbon nanotube composite, *Phys. Chem. Earth* 66 (2013) 157–166.
- [50] R. Ahmad, S. Haseeb, Adsorption of Pb(II) on menthe piperita carbon (MTC) in single and quaternary systems, *Arab. J. Chem.* (in press) (2012), doi: [10.1016/j.arabjc.2012.09.013](https://doi.org/10.1016/j.arabjc.2012.09.013).
- [51] L. Svecova, M. Spanelova, M. Kubal, E. Guibal, Cadmium, lead and mercury biosorption on waste fungal biomass issued from fermentation industry. I. Equilibrium studies, *Sep. Purif. Technol.* 52 (2006) 142–153.
- [52] M.D. Meitei, M.N.V. Prasad, Lead(II) and cadmium(II) biosorption on *Spirodela polyrhiza* (L.) Schleiden biomass, *J. Environ. Chem. Eng.* 1 (2013) 200–207.
- [53] N. Pourreza, T. Naghdi, Silicon carbide nanoparticles as an adsorbent for solid phase extraction of lead and determination by flame atomic absorption spectrometry, *J. Ind. Eng. Chem* 20 (2014) 3502–3506.
- [54] W. Zou, R. Han, Z. Chen, J. Shi, L. Liu, Characterization and properties of manganese oxide coated zeolite as adsorbent for removal of copper(ii) and lead(ii) ions from solution, *J. Chem. Eng. Data* 51 (2006) 534–541.
- [55] K. Rout, M. Mohapatra, S. Anand, A critical analysis of cation adsorption from single and binary solutions on low surface area MnO₂, *Appl. Surf. Sci.* 270 (2013) 205–218.
- [56] X.L. Tan, P.P. Chang, Q.H. Fan, X.S. Zhou, S.M. Yu, W.S. Wu, X.K. Wang, Sorption of Pb(II) on Na-rectorite: Effects of pH, ionic strength, temperature, soil humic acid and fulvic acid, *Colloids Surf., A* 328 (2008) 8–14.
- [57] X. Yongjie, H. Haobo, Z. Shujing, Competitive adsorption of copper(II), cadmium(II), lead(II) and zinc(II) onto basic oxygen furnace slag, *J. Hazard. Mater.* 162 (2009) 391–401.
- [58] M. Namazian, S. Halvani, Calculations of pKa values of carboxylic acids in aqueous solution using density functional theory, *J. Chem. Thermodyn.* 38 (2006) 1495–1502.
- [59] F.Z. Erdemgil, S. Sanli, N. Sanli, G. Ozkan, J. Barbosa, J. Guiteras, J.L. Beltran, Determination of pKa values of some hydroxylated benzoic acids in methanol-water binary mixtures by LC methodology and potentiometry, *Talanta* 72 (2007) 489–496.
- [60] M.J. Baniamerian, S.E. Moradi, A. Noori, H. Salahi, The effect of surface modification on heavy metal ion removal from water by carbon nanoporous adsorbent, *Appl. Surf. Sci.* 256 (2009) 1347–1354.
- [61] T. Depci, A.R. Kul, Y. Önal, Competitive adsorption of lead and zinc from aqueous solution on activated carbon prepared from Van apple pulp: Study in single- and multi-solute systems, *Chem. Eng. J.* 200–202 (2012) 224–236.
- [62] L. Semerjian, Equilibrium and kinetics of cadmium adsorption from aqueous solutions using untreated *Pinus halepensis* sawdust, *J. Hazard. Mater.* 173 (2010) 236–242.
- [63] S.J. Allen, G. Mckay, J.F. Porter, Adsorption isotherm models for basic dye adsorption by peat in single and binary component systems, *J. Colloid Interface Sci.* 280 (2004) 322–333.
- [64] G. Limousin, J. Gaudet, L. Charlet, S. Szenknect, V. Barthès, M. Krimissa, Sorption isotherms: A review on physical bases, modeling and measurement, *Appl. Geochem.* 22 (2007) 249–275.
- [65] K.Y. Foo, B.H. Hameed, Insights into the modeling of adsorption isotherm systems, *Chem. Eng. J.* 156 (2010) 2–10.
- [66] A.O. Dada, A.P. Olalekan, A.M. Olatunya, O. Dada, Langmuir, Freundlich, Temkin and Dubinin-Radushkevich isotherms studies of equilibrium sorption of Zn²⁺ onto phosphoric acid modified rice husk, *IOSR J. Appl. Chem.* 3 (2012) 38–45.
- [67] E. Ayranci, O. Duman, Adsorption behaviors of some phenolic compounds onto high specific area activated carbon cloth, *J. Hazard. Mater. B* 124 (2005) 125–132.
- [68] A.S.A. Khan, Theory of adsorption equilibria analysis based on general equilibrium constant expression, *Turk. J. Chem.* 36 (2012) 219–231.
- [69] E. Voudrias, F. Fytianos, E. Bozani, Sorption description isotherms of dyes from aqueous solutions and waste waters with different sorbent materials, *Global Nest Int. J.* 4 (2002) 75–83.
- [70] S. Goldberg, Equations and models describing adsorption processes in soils, *Soil Sci. Soc. Am.* (2005) 489–517.
- [71] A. Dąbrowski, Adsorption—From theory to practice, *Adv. Colloid Interface Sci.* 93 (2001) 135–224.
- [72] A. Günay, E. Arslankaya, İsmail Tosun, Lead removal from aqueous solution by natural and pretreated clinoptilolite: Adsorption equilibrium and kinetics, *J. Hazard. Mater.* 146 (2007) 362–371.
- [73] R.A.K. Rao, M.A. Khan, B.H. Jeon, Utilization of carbon derived from mustard oil cake (CMOC) for the removal of bivalent metal ions: Effect of anionic surfactant on the removal and recovery, *J. Hazard. Mater.* 173 (2010) 273–282.
- [74] R. Subha, C. Namasivayam, Kinetics and isotherm studies for the adsorption of phenol using low cost micro porous ZnCl₂ activated coir pith carbon, *Can. J. Civil Eng.* 36 (2009) 148–159.

- [75] R.S. Azarudeen, R. Subha, D. Jeyakumar, A.R. Burkanudeen, Batch separation studies for the removal of heavy metal ions using a chelating terpolymer: Synthesis, characterization and isotherm models, *Sep. Purif. Technol.* 116 (2013) 366–377.
- [76] M. Li, Y. Wang, Q. Liu, Q. Li, Y. Cheng, Y. Zheng, T. Xi, S. Wei, In situ synthesis and biocompatibility of nano hydroxyapatite on pristine and chitosan functionalized graphene oxide, *J. Mater. Chem. B* 1 (2013) 475–484.
- [77] Y.S. Ho, G. McKay, The kinetics of sorption of basic dyes from aqueous solution by sphagnum moss peat, *Can. J. Chem. Eng.* 76 (1998) 822–827.
- [78] Y.S. Ho, Removal of copper ions from aqueous solution by tree fern, *Water Res.* 37 (2003) 2323–2330.
- [79] Z.Y. Yao, J.H. Qi, L.H. Wang, Equilibrium, kinetic and thermodynamic studies on the biosorption of Cu(II) onto chestnut shell, *J. Hazard. Mater.* 174 (2010) 137–143.
- [80] B. Volesky, Sorption and biosorption, BV. Sorbex Inc. Publications, Quebec, 2003, pp. 183–185.
- [81] I. Ghodbane, O. Hamdaoui, Removal of mercury(II) from aqueous media using eucalyptus bark: Kinetic and equilibrium studies, *J. Hazard. Mater.* 160 (2008) 301–309.
- [82] V.K. Gupta, A.K. Shrivastava, N. Jain, Biosorption of chromium(VI) from aqueous solutions by green algae *Spirogyra* species, *Water Res.* 35 (2001) 4079–4085.
- [83] T. Kwon, C. Jeon, Desorption and regeneration characteristics for previously adsorbed indium ions to phosphorylated sawdust, *Environ. Eng. Res.* 17 (2012) 65–67.
- [84] P. Liu, L. Jiang, L. Zhu, A. Wang, Novel approach for attapulgite/poly(acrylic acid) (ATP/PAA) nanocomposite microgels as selective adsorbent for Pb(II) Ion, *React. Funct. Poly.* 74 (2014) 72–80.